

## Multiscale simulations of damage of perfect crystal Cu at high strain rates

S RAWAT<sup>1</sup>, M WARRIER<sup>2,\*</sup>, S CHATURVEDI<sup>2</sup> and V R IKKURTHI<sup>2</sup>

<sup>1</sup>Refueling Technology Division, Bhabha Atomic Research Centre, Mumbai 400 085, India

<sup>2</sup>Computational Analysis Division, Bhabha Atomic Research Centre,  
Visakhapatnam 530 012, India

\*Corresponding author. E-mail: manoj.warrier@gmail.com

DOI: 10.1007/s12043-014-0792-8; ePublication: 22 July 2014

**Abstract.** We use the molecular dynamics code, large-scale atomic/molecular massively parallel simulator (LAMMPS), to simulate high strain rate triaxial deformation of crystal copper to understand void nucleation and growth (NAG) within the framework of an experimentally fitted macroscopic NAG model for polycrystals (also known as DFRAC model). It is seen that void NAG at the atomistic scales for crystal copper (Cu) has the same qualitative behaviour as the DFRAC model, albeit with a different set of parameters. The effect of material temperature on the nucleation and growth of voids is studied. As the temperature increases, there is a steady decrease in the void NAG thresholds and close to the melting point of Cu, a double-dip in the pressure–time profile is observed. Analysis of this double-dip shows disappearance of the long-range order due to the creation of stacking faults and the system no longer has a face centred cubic (fcc) structure. Molecular dynamics simulation of shock in crystal Cu at strain rates high enough to cause spallation of crystal Cu are then carried out to validate the void NAG parameters. We show that the pre-history of the material affects the void nucleation threshold of the material. We also simulate high-strain-rate triaxial deformation of crystal Cu with defects and obtain void NAG parameters. The parameters are then used in a macroscale hydrodynamic simulation to obtain spallation threshold of realistic crystal Cu. It is seen that our results match experimental results within the limit of 20% error.

**Keywords.** Single crystal copper; spallation; multiscale; DFRAC model; void nucleation.

**PACS Nos** 61.72.Qq; 62.20.–F; 62.20.–M; 62.20.mm

### 1. Introduction

Solid fracture under high strain deformation is of interest for high velocity impact and penetration problems. It is known that nucleation, growth and coalescence of voids lead to the failure of the ductile solid materials [1]. There are various methods to produce high strain rates in materials, e.g., plate impact [2], laser blow-off [3] etc. Laser-induced shock waves in materials can create high strain rates of the order of  $(10^7-10^{10})/s$  in the material

[4–7]. Dynamics of atoms/molecules subjected to such high strain rates can be computationally investigated by molecular dynamics which is well suited to study many millions of atoms for several nanoseconds. The information gleaned at the atomistic scales can be used as parameters in simulations at macroscale within a multiscale modelling paradigm.

There are three inputs to the hydrodynamic simulations of fracture at macroscale: (a) an equation of state, (b) a model to predict strength of the material and (c) a dynamic fracture model, e.g., nucleation and growth (NAG) model. In this paper, we simulate high-strain-rate triaxial deformation of single-crystal Cu using molecular dynamics and obtain the best-fit NAG parameters for perfect crystal Cu and crystal Cu with defects. Then we use these best-fit NAG parameters for crystal Cu in a macroscopic hydrodynamic simulation, using one-dimensional Lagrangian code, to generate spall data for single crystal Cu.

## 2. Nucleation and growth (NAG) model

The NAG model (also known as DFRAC model) developed at Stanford Research Institute [1,14] is a microphysical model which describes the fracture processes that occur as nucleation and growth of voids in ductile materials.

In this model, new voids are created if the tensile pressure  $P_s$  in the solid material exceeds the nucleation threshold  $P_{n0}$  of the material and existing voids grow if the tensile pressure in the material exceeds the threshold for void growth  $P_{g0}$ . The total void volume due to nucleation and growth of voids at the end of the time interval is given by

$$V_v = 8\pi \Delta t R_n^3 \dot{N}_0 \exp\left[\frac{P_s - P_{n0}}{P_1}\right] + V_{v0} \exp\left[\frac{3}{4} \left(\frac{P_s - P_{g0}}{\eta}\right) \Delta t\right], \quad (1)$$

where  $\dot{N}_0$  is the threshold nucleation rate and  $P_1$  is the pressure sensitivity for nucleation. Both  $\dot{N}_0$  and  $P_1$  are material constants.  $P_s$  is the tensile pressure in the system,  $V_{v0}$  is the void volume at the beginning of the time interval,  $\eta$  is the material viscosity and  $R_n$  is a material parameter known as nucleation size parameter.

## 3. Molecular dynamics simulation

### 3.1 High-strain-rate triaxial deformation of crystal Cu

3.1.1 *Initial set-up.* Isotropic tension in single-crystal Cu has been simulated using the molecular dynamics code, large-scale atomic/molecular massively parallel simulator (LAMMPS) [8]. A cubic simulation cell containing a certain number of atoms  $N$  ( $4 \times 10^6$  atoms,  $100 \times 100 \times 100$  unit cells) is created by replicating fcc unit cells along the  $x$ -,  $y$ -, and  $z$ -axes.

We have used the embedded-atom method [9,10] potential parameters generated by Foiles *et al* [11] in our simulation. The equations of motion are integrated with a time-step of 1 femtosecond (fs) using the velocity-Verlet algorithm since, the results do not change for time-steps  $\leq 1$  fs. Periodic boundary conditions are used in all three directions for this study. The thermal velocities of all the atoms have been initialized using a Gaussian distribution at a temperature of 300 K. To relax the system to minimum energy, NPT

simulation is performed at 0 bar and 300 K. Nose–Hoover thermostat and barostat [12,13] have been used to control the temperature and pressure.

After pressure and temperature stabilize, the barostat is turned off and high-strain-rate ( $5 \times 10^9$  /s) triaxial expansion is applied at constant temperature.

**3.1.2 Pressure–time profile and NAG parameters for single-crystal Cu.** Internal pressure as a function of time for single-crystal Cu triaxially deformed at  $5 \times 10^9$  /s strain rate is shown in figure 1a. It is seen in the figure that the tensile pressure increases continuously upto a time point and then turns around at 168 kbar. The turn-around in pressure corresponds to the NAG of voids. The rapid reduction in pressure after turn-around is due to the growth and coalescence of voids. After that, the pressure fluctuates around some negative value corresponding to the growth threshold of voids.

For a given (assumed) set of NAG parameters, the known pressure–time profile can be used to get the total void volume (eq. (1)) due to NAG of voids. We have developed a post-processor which computes void volume in the domain using atomic coordinates. The details of the post-processor are described in [14]. The void volume obtained from NAG model (eq. (1)) is then compared with that computed using the post-processor. An overall minimization procedure is then used to get best-fit NAG parameters.

The comparison of void volume fraction obtained by NAG model and that computed using post-processor is shown in figure 1b. In figure 1b, it is seen that there is a qualitative match of NAG model. The best-fit NAG parameters for single-crystal Cu at 300 K [14] along with polycrystalline Cu [1] are shown in table 1.

From table 1, it is seen that the void nucleation threshold for crystal Cu is very high compared to oxygen-free high thermal conductivity (OFHC) copper which is reasonable because in polycrystalline Cu there are many weak points, e.g., grain boundaries, which lower the threshold for void nucleation. The value of pressure sensitivity for crystal Cu is very low compared to polycrystalline Cu which means that the nucleation rate in single crystals is much more sensitive to pressure than that for polycrystalline Cu. The lower value of material viscosity for crystal Cu compared to polycrystalline Cu indicates rapid

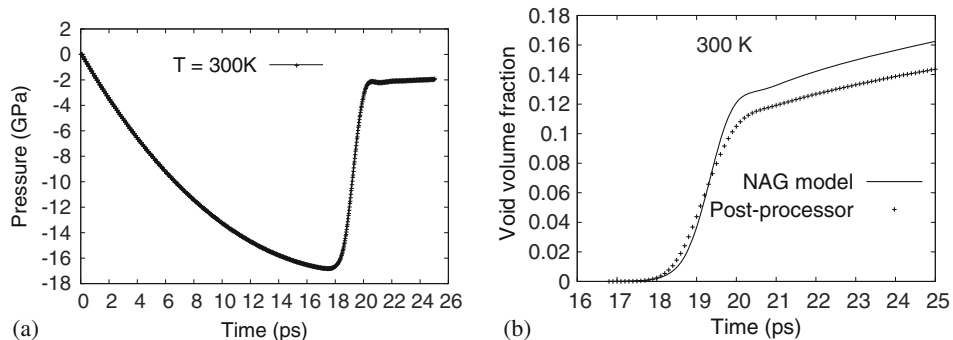


**Figure 1.** (a) Internal pressure as a function of time for perfect single-crystal Cu triaxially deformed at  $5 \times 10^9$  /s strain rate at 300 K. (b) Qualitative match of NAG model.

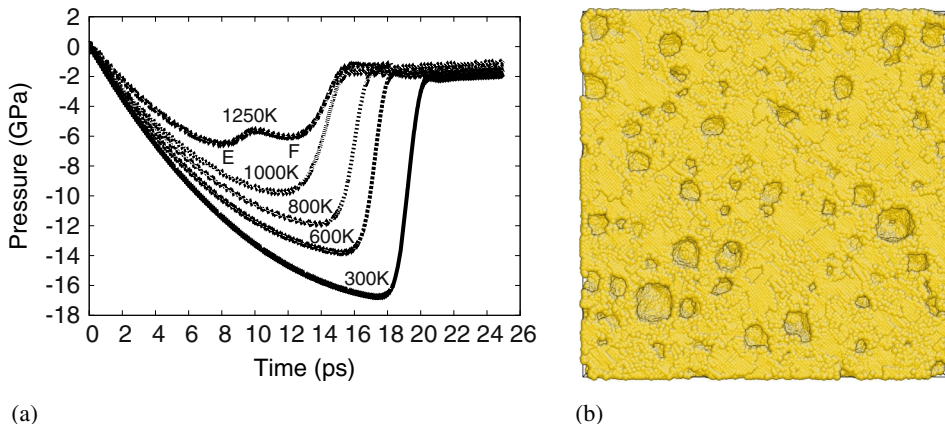
**Table 1.** Best-fit NAG parameters for perfect single-crystal Cu triaxially deformed at  $5 \times 10^9$  /s strain rate at 300 K.

NAG parameters	$P_{n0}$ (kbar)	$P_1$ (kbar)	$\dot{N}_0$ ( $\text{m}^{-3} \text{s}^{-1}$ )	$P_{g0}$ (kbar)	$\eta$ (bar s)
Single-crystal Cu	-160.4	-0.167	$7.1 \times 10^{18}$	-21.2	$3.4 \times 10^{-8}$
OFHC Cu [1]	-5.0	2.0	$2.8 \times 10^{18}$	-5.0	$7.5 \times 10^{-5}$

growth of voids once the nucleation threshold is crossed. The growth threshold in table 1 corresponds to the tensile pressure fluctuating around a small negative value (figure 1).

**3.1.3 Effect of temperature on the NAG of voids.** The comparison of internal pressure as a function of time for single-crystal Cu triaxially deformed at  $5 \times 10^9$  /s strain rate with 300, 600, 800, 1000 and 1250 K as initial temperatures is shown in figure 2. In this figure, it is seen that there is a monotonic decrease in the NAG thresholds of voids with increase in temperature. At 1250 K, there is a double dip in the pressure–time profile. The analysis by radial distribution function, centrosymmetry parameter, structure factor and common neighbour analysis [14] shows that the first minimum (point E) corresponds to the loss of long-range order and the system no longer has an fcc structure. The second minimum (point F) corresponds to the NAG of voids.

**3.1.4 NAG parameters for single-crystal Cu with defects.** We have simulated triaxial deformation of single-crystal Cu with various kinds of defects such as dislocations, stacking faults and vacancies at  $5 \times 10^9$  /s strain rate at 300 K. For example, to create an edge

**Figure 2.** (a) Internal pressure for single-crystal Cu deformed at  $5 \times 10^9$  /s strain rate with different initial temperatures. (b) Snapshot at 20 ps for the case of 300 K.

dislocation, we remove atoms lying on a half-plane in the centre of the  $100 \times 100 \times 100$  unit cells and carry out NPT MD simulations. This produces an edge dislocation with the atoms in the neighbourhood properly shifted and equilibrated. We then repeat the triaxial deformation and obtain the best-fit NAG parameters as discussed in §3.1.2. The best-fit NAG parameters for single-crystal Cu with such a pre-existing edge dislocation (half plane missing) is shown in table 2. Table 2 shows that there is a large reduction in void nucleation threshold of crystal Cu with the edge dislocation defect compared to that of perfect crystal Cu (table 1).

### 3.2 High-velocity impact of Cu plates

3.2.1 *Initial set-up.* To simulate high-velocity impact of Cu plates, a cubic cell containing  $N = 1.08 \times 10^6$  atoms is created by replicating  $300 \times 30 \times 30$  unit cells along  $x$ -,  $y$ - and  $z$ -axes. Free boundary conditions are used along the  $x$ -direction (shock direction) and periodic boundary conditions are used along transverse directions ( $y$ - and  $z$ -directions). Thickness of the Cu flyer is  $361.5 \text{ \AA}$  (100 unit cells) and that of the target is  $723 \text{ \AA}$  (200 unit cells). Impact is done along  $x$ -direction with 1.0 and 1.1 km/s impact velocities.

To analyse the shock wave propagation, the system is divided into bins along the  $x$ -axis. The width of the bin used to analyse the shock wave is  $10.83 \text{ \AA}$  (3 unit cells).

#### 3.2.2 Results and discussion

- (1) *Impact at 1.1 km/s:* the impact of Cu flyer onto the Cu target produces compressive stress waves which propagate toward the respective free surfaces of the flyer and the target plates. When they reach the respective free surfaces of the flyer and the target, they get reflected as release waves and interact at some location inside the target. The interaction of release waves leads to tension and if the tension created exceeds the tensile strength of the material, nucleation, growth and coalescence of voids take place leading to spall of the material. The internal pressure as a function of time in the spall region of the target for the impact at an impact velocity of 1.1 km/s is shown in figure 3a. It can be seen from this figure that the most negative pressure in the region where spall occurs is 160 kbar. This validates the void nucleation threshold obtained for perfect crystal Cu triaxially deformed at  $5 \times 10^9$  /s strain rate (§3.1.2). The flat region in figure 3a around zero after point Q indicates the spall of the material. The detailed results and discussion for the impact of Cu plates at 1.1 km/s impact velocity are described in [15].

**Table 2.** Best-fit NAG parameters for single-crystal Cu with a pre-existing edge dislocation. Strain rate applied is  $5 \times 10^9$  /s.

NAG parameters	$P_{n0}$ (kbar)	$P_1$ (kbar)	$\dot{N}_0$ ( $\text{m}^{-3} \text{ s}^{-1}$ )	$P_{g0}$ (kbar)	$\eta$ (bar s)
Single-crystal Cu with a pre-existing edge dislocation	-42.7	-3.85	$2.73 \times 10^{20}$	-47.0	$2.0 \times 10^{-7}$

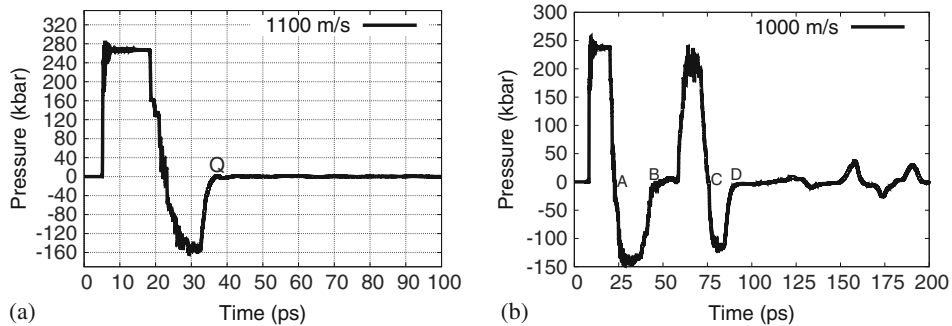


**Figure 3.** (a) Pressure in the spall region as a function of time for the impact of Cu plates at an impact velocity of 1.1 km/s. (b) Pressure in the void nucleation region as a function of time for the impact of Cu plates at an impact velocity of 1.0 km/s.

- (2) *Impact at 1.0 km/s:* pressure as a function of time in the region where voids nucleate and grow is shown in figure 3b. It is seen that the most negative pressure (region AB) corresponding to first traversal of the shock is less than the void nucleation threshold (160 kbar) and therefore, does not lead to the nucleation of voids. This can be seen in figure 3b where pressure does not flatten off around zero, which is the signature of nucleation of voids. The void NAG occurs corresponding to the second traversal of shock at lower value of tensile pressure (region CD). The reason for nucleation of voids at lower value of tensile pressure is that the tension (region AB) created corresponding to the first traversal of shock creates various kinds of defects which become void nucleation sites during the tension (region CD) due to second traversal of shock. This results in the nucleation of voids at lower value of tensile pressure. This means that pre-history of the material under study affects the void nucleation threshold of the material. A detailed analysis of the results is described in [15].

#### 4. Hydrodynamic simulation

We have obtained NAG parameters for single-crystal Cu with different kinds of defects, such as dislocations, stacking faults and vacancies. These parameters are then used in a macroscale hydrodynamic simulation, using a one-dimensional Lagrangian hydrocode, to generate spall data. An impact-loaded spallation experiment involving single-crystal Cu [16] has been simulated using the code. To compute pressure in the computational cells, a six-parameter equation of state [18] for Cu has been used. We have used Steinberg–Guinan dynamic strength model [19] to compute the variation of yield strength and shear modulus with pressure, temperature and plastic strain in the material. The DFRAC model, with model parameters obtained from atomistic simulations (§3.1.4), has been used to compute damage or porosity. The free surface velocity–time history obtained from simulation is used to derive spall threshold and scab thickness [17]. Our results are compared with the published experimental data for single-crystal Cu [16].

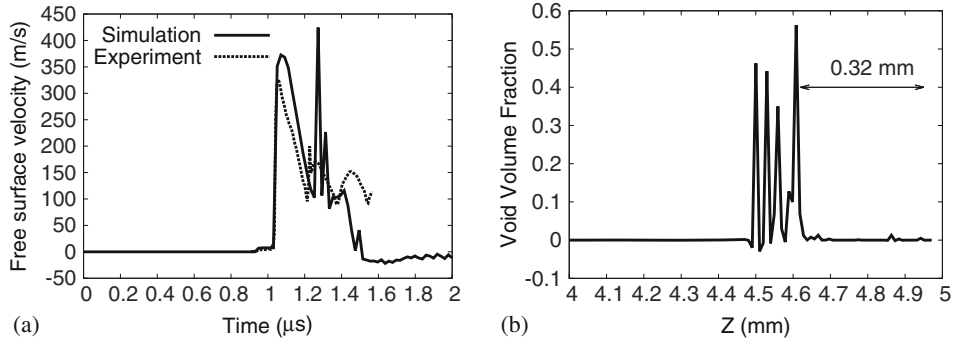


**Figure 4.** (a) Comparison of free surface velocities obtained from the experiment and simulation. (b) Void volume fraction as a function of target thickness. Aluminum flyer impacts single-crystal Cu target with an impact velocity of 660 m/s.

**Table 3.** Comparison of spall strength and spall thickness for single-crystal Cu obtained from hydrodynamic simulations with the experimental values.

Parameters	Simulation	Experiment [16]
Spall strength (kbar)	48.0	$39.5 \pm 0.1$
Spall thickness (mm)	0.32	0.3 (10%)

For the type of defect that produces the best match, the edge dislocation, the comparison of free surface velocities of the target and the void volume fraction as a function of target thickness are shown in figures 4a and 4b, respectively. The comparison of the simulation results with the experimental values is shown in table 3.

We find that our results match with the experimental results within an error of 20% for pre-existing edge dislocation in single-crystal Cu.

## 5. Conclusion

We have performed molecular dynamics simulations to study NAG of voids in single-crystal Cu and best-fit NAG parameters were obtained for perfect crystal Cu and crystal Cu with defects. We found that the pre-existing defects lower the void nucleation threshold. Material temperature affects the NAG thresholds of voids and a monotonic decrease in the thresholds for NAG of voids with increase in temperature was observed. The 1.1 km/s impact simulations validated the void nucleation threshold obtained under high-strain-rate triaxial deformation of crystal Cu. Impact of Cu plates at an impact velocity of 1.0 km/s showed that the pre-history of the material affects the void nucleation threshold. The void NAG parameters obtained by atomistic simulations for single-crystal Cu were used in hydrodynamic simulations. We found that our results match with the experimental results within the limit of 20% error for pre-existing edge dislocation in single-crystal Cu.

## References

- [1] D R Curran, L Seaman and D A Shockey, *Phys. Rep.* **147(5,6)**, 253 (1987)
- [2] R W Minich, J U Cazamias, M Kumar and A J Schwartz, *Metall. Mater. Trans. A* **35**, 2663 (2004)
- [3] H Tamura, T Kohama, K Kondo and M Yoshida, *J. Appl. Phys.* **89**, 3520 (2001)
- [4] E Moshe et al, *J. Appl. Phys.* **86(8)**, 4242 (1999)
- [5] E Dekel, S Eliezer, Z Henis, E Moshe, A Ludmirsky and I B Goldberg, *J. Appl. Phys.* **84(9)**, 4851 (1998)
- [6] S Eliezer, I Gilath and T Bar-Noy, *J. Appl. Phys.* **67(2)**, 715 (1990)
- [7] W J Murphy et al, *J. Phys.: Condens. Matter* **22**, 065404 (2010)
- [8] S Plimpton, *J. Comput. Phys.* **117**, 1 (1995)
- [9] M S Daw and M I Baskes, *Phys. Rev. Lett.* **50**, 1285 (1983)
- [10] M S Daw and M I Baskes, *Phys. Rev. B* **29**, 6443 (1984)
- [11] S M Foiles, M I Baskes and M S Daw, *Phys. Rev. B* **33**, 7983 (1986)
- [12] W G Hoover, *Phys. Rev. A* **31**, 1695 (1985)
- [13] W G Hoover, *Phys. Rev. A* **34**, 2499 (1986)
- [14] S Rawat, M Warriar, S Chaturvedi and V M Chavan, *Modell. Simul. Mater. Sci. Eng.* **19**, 025007 (2011)
- [15] S Rawat, M Warriar, S Chaturvedi and V M Chavan, *Modell. Simul. Mater. Sci. Eng.* **20**, 015012 (2012)
- [16] T H Antoun, L Seaman and D R Curran, Tech. Rep. No. DSWA-TR-96-77-V2 (Defence Special Weapons Agency, Alexandria, VA, 1998)
- [17] V R Ikkurthi and S Chaturvedi, *Int. J. Impact Eng.* **30**, 275 (2004) and references therein
- [18] S Eliezer, A Ghatak, H Hora and E Teller, *An introduction to equations of state, theory and applications* (Cambridge University Press, Cambridge, 1986)
- [19] D J Steinberg, S G Cochran and M W Guinan, *J. Appl. Phys.* **51(3)**, 1498 (1980)